

Contrasting Formation of a (Phenylthio)phosphinimine and (Phenylthio)phosphazide. Synthesis of Metal Complexes

Luc LePichon and Douglas W. Stephan*

School of Physical Sciences, Chemistry and Biochemistry, University of Windsor, Windsor, Ontario, Canada N9B 3P4

Received November 17, 2000

Much of what is known about phosphinimide and phosphinimine complexes of the transition and main-group metals arises from the numerous structural studies described by Dehnicke and co-workers.^{1,2} While some studies of the chemistry of the complexes of these ligands have appeared, in general, such systems are unexplored. Recently, we have demonstrated that early metal–phosphinimide species can act as highly active olefin polymerization catalysts.^{3,4} Although Reetz et al.⁵ have begun to employ chiral bidentate bisphosphinimines in asymmetric synthesis, in general, heteroatomic bidentate ligands containing phosphinimine² and phosphazide^{6–8} donors have received little attention.^{9,10} In efforts to develop the new potentially bidentate ligand systems for use with late transition metals, we have investigated the synthesis of phosphinimine and phosphazide derivatives of trialkylphosphines that incorporate thioether units. The structures of Ni and Fe complexes of these ligands are presented, and the implications for the development of new bidentate phosphinimine-based ligand systems are considered.

Experimental Section

General Data. All preparations were done under an atmosphere of dry, O₂-free N₂ employing both Schlenk line techniques and Innovative Technologies or Vacuum Atmospheres inert atmosphere gloveboxes. Solvents were purified employing Grubbs type column systems manufactured by Innovative Technology. All organic reagents were purified by conventional methods. Guelph Chemical Laboratories Inc. of Guelph, Ontario performed combustion analyses. N₃CH₂SPh, *t*-Bu₃P, *i*-Pr₃P, and anhydrous FeCl₂ were purchased from the Aldrich Chemical Co. NiCl₂(DME) was purchased from the Strem Chemical Co.

Synthesis of *i*-Pr₃PNCH₂SPh (1) and *t*-Bu₃PN₃CH₂SPh (2). These compounds were prepared in a similar fashion using the appropriate phosphine, and thus only one preparation is detailed. N₃CH₂SPh (347 mg, 2.1 mmol) was added to *t*-Bu₃P (405 mg, 2 mmol), and white solid appeared immediately. The reaction mixture was heated at 90 °C

Table 1. Crystallographic Parameters^a

| | 3 | 4 | 5 |
|---|---|--|--|
| formula | C ₁₆ H ₂₈ Cl ₂ FeNPS | C ₄₁ H ₆₄ Cl ₂ N ₆ NiP ₂ S ₂ | C ₃₈ H ₆₇ Cl ₂ FeN ₆ P ₂ S ₂ |
| formula weight | 424.17 | 896.65 | 860.79 |
| <i>a</i> (Å) | 9.32850(10) | 21.5918(2) | 13.917(5) |
| <i>b</i> (Å) | 15.2783(3) | 10.60690(10) | 21.409(7) |
| <i>c</i> (Å) | 15.0720(2) | 22.79520(10) | 15.513(5) |
| β (deg) | 102.1040(10) | 106.3120(10) | 93.821(8) |
| cryst syst | monoclinic | monoclinic | monoclinic |
| space group | <i>P</i> 2(1)/ <i>c</i> | <i>P</i> 2(1)/ <i>c</i> | <i>P</i> 2(1)/ <i>n</i> |
| Volume (Å ³) | 2100.36(5) | 5010.45(7) | 4612(3) |
| <i>D</i> _{calcd} (g cm ⁻³) | 1.341 | 1.189 | 1.240 |
| <i>Z</i> | 4 | 4 | 2 |
| abs coeff, μ , mm ⁻¹ | 1.144 | 0.674 | 0.635 |
| R (%) | 0.0478 | 0.0869 | 0.0534 |
| Rw (%) | 0.1202 | 0.1957 | 0.1554 |

^a All data collected at 24 °C with Mo K α radiation ($\lambda = 0.71069$ Å), $R = \sum ||F_o| - |F_c|| / \sum |F_o|$, $R_w = [\sum (\omega F_o^2 - F_c^2)^2] / \sum (\omega F_o^2)^2$]^{0.5}.

and stirred for 30 min. The solution was then cooled to room temperature. The white solid formed was washed with hexane and dried under a vacuum; 540 mg (73%) of **2** was obtained. **1.** reaction at 25 °C, yield: 98%. ¹H NMR (C₆D₆): δ 7.80–6.93 (5H, Ph), 5.25(d, 2H, CH₂, $J_{PH} = 25$ Hz), 1.88 (sept, $J_{HH} = 7.5$ Hz, $J_{PH} = 3.0$ Hz, 3H) 0.98 (dd, 18H). ¹³C{¹H} NMR (C₆D₆): δ 141.4, 130.0, 129.0, 125.1 (Ph), 56.9 (d, CH₂, $J_{PC} = 8.6$ Hz), 24.9 (d, CH, $J_{PC} = 57.6$ Hz), 17.7 (d, CH₃, $J_{PC} = 2.2$ Hz). ³¹P{¹H} NMR (C₆D₆): δ 32.8. **2.** No evolution of N₂ was observed in this case. ¹H NMR (C₆D₆): δ 7.59–6.88 (5H, Ph), 5.28 (s 2H, CH₂), 1.17 (d, 27H, CH₃, $J_{PH} = 10$ Hz). ¹³C{¹H} NMR (C₆D₆): δ 139.0, 130.2, 129.2, 125.9 (Ph), 64.4 (CH₂), 40.4 (d, P–C, $J_{PC} = 40$ Hz), 30.2 (CH₃). ³¹P{¹H} NMR (C₆D₆): δ 50.9. EA Calcd. for C₁₉H₃₄N₃PS: C, 62.09; H, 9.32; N, 11.43. Found: C, 61.96; H, 9.70; N, 11.47.

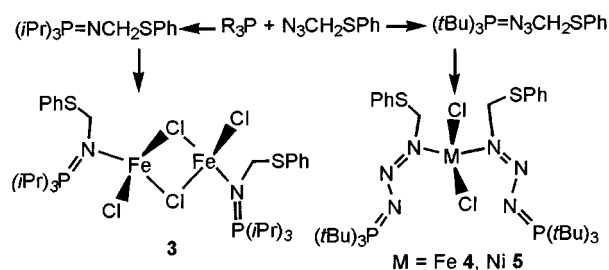
Synthesis of [(*i*-Pr₃PNCH₂SPh)FeCl(μ -Cl)]₂ (3). A solution of **1** (100 mg, 0.34 mmol) in 5 mL of toluene was added to a suspension of FeCl₂ (43 mg, 0.34 mmol) in 5 mL of toluene. The reaction mixture was stirred for 20 h. The toluene was removed in vacuo to give a pale yellow precipitate. A pale yellow solution was extracted with dichloromethane. Upon standing, 30 mg of crystals of **3** were obtained (21%). EA Calcd. for C₃₂H₅₆Cl₄Fe₂N₆P₂S₂: C, 45.30; H, 6.65; N, 3.30. Found: C, 45.41; H, 6.93; N, 3.25.

Synthesis of (*t*-Bu₃PN₃CH₂SPh)₂NiCl₂ (4) and (*t*-Bu₃PN₃CH₂SPh)₂FeCl₂ (5). These compounds were prepared in a similar fashion using FeCl₂ or NiCl₂(DME), and thus only one preparation is detailed. FeCl₂ (32 mg, 0.25 mmol) was added to a solution of **2** (184 mg, 0.50 mmol) in 2.5 mL of toluene. The reaction mixture was stirred for 20 h at room temperature. An orange complex formed. The solvent was removed, and the orange powder was washed with hexane. After recrystallization in a mixture of toluene/hexane, 190 mg of orange crystals of **5** (88%) were isolated. EA Calcd. for C₃₈H₆₈N₆P₂S₂FeCl₂: C, 52.96; H, 7.95; N, 9.75. Found: C, 52.78; H, 8.36; N, 9.61. **4.** Pink solid, yield: 85%. EA. Calcd. for C₃₈H₆₈N₆P₂S₂NiCl₂+0.3C₆H₆: C, 53.83; H, 7.92; N, 9.46. Found: C, 53.82; H, 8.26; N, 9.44.

X-ray Data Collection and Reduction. The crystals were manipulated and mounted in capillaries in a glovebox. Diffraction experiments were performed on a Siemens SMART System CCD diffractometer, collecting a hemisphere of data in 1329 frames with 10 s exposure times. Crystal data are summarized in Table 1. A measure of decay was obtained by re-collecting the first 50 frames of each data set. The intensities of reflections within these frames showed no statistically significant change over the duration of the data collections. The data were processed using the SAINT and XPREP processing packages. An empirical absorption correction based on redundant data was applied to each data set. Subsequent solution and refinement was performed

- (1) Dehnicke, K.; Weller, F. *Coord. Chem. Rev.* **1997**, *158*, 103–169.
- (2) Dehnicke, K.; Krieger, M.; Massa, W. *Coord. Chem. Rev.* **1999**, *182*, 19–65.
- (3) Stephan, D. W.; Guerin, F.; Spence, R. E. v. H.; Koch, L.; Gao, X.; Brown, S. J.; Swabey, J. W.; Wang, Q.; Xu, W.; Zoricak, P.; Harrison, D. G. *Organometallics* **1999**, *18*, 2046–2048.
- (4) Stephan, D. W.; Stewart, J. C.; Guerin, F.; Spence, R. E. v. H.; Xu, W.; Harrison, D. G. *Organometallics* **1999**, *18*, 1116–1118.
- (5) Reetz, M. T.; Bohres, E.; Goddard, R. *Chem. Commun.* **1998**, *008*, 935–936.
- (6) Hillhouse, G. L.; Haymore, B. L. *J. Organomet. Chem.* **1978**, *162*, C23–C26.
- (7) Hillhouse, G.; Goeden, G. V.; Haymore, B. L. *Inorg. Chem.* **1982**, *21*, 2064–2071.
- (8) Bieger, K.; Bouhadir, G.; Reau, R.; Dahan, F.; Bertrand, G. *J. Am. Chem. Soc.* **1996**, *118*, 1038–1044.
- (9) Katti, K. V.; Cavell, R. G. *Organometallics* **1991**, *10*, 539–541.
- (10) Katti, K. V.; Santarsiero, B. D.; Pinkerton, A. A.; Cavell, R. G. *Inorg. Chem.* **1993**, *32*, 5919–5925.

Scheme 1



using the SHELXTL solution package. The reflections with $F_o^2 > 3\sigma F_o^2$ were used in the refinements.

Structure Solution and Refinement. Non-hydrogen atomic scattering factors were taken from the literature tabulations.¹¹ The heavy atom positions were determined using direct methods, employing the SHELXTL direct methods routines. The remaining non-hydrogen atoms were located from successive difference Fourier map calculations. The refinements were carried out by using full-matrix least squares techniques on F , minimizing the function $\omega(|F_o| - |F_c|)^2$, where the weight ω is defined as $4F_o^2/2\sigma(F_o^2)$, and F_o and F_c are the observed and calculated structure factor amplitudes. In the final cycles of each refinement, all non-hydrogen atoms were assigned anisotropic temperature factors. Carbon bound hydrogen atom positions were calculated and allowed to ride on the carbon to which they are bonded, assuming a C–H bond length of 0.95 Å. Hydrogen atom temperature factors were fixed at 1.10 times the isotropic temperature factor of the carbon atom to which they are bonded. In the case of **4**, a two-site disorder of one of the thiophenol groups was modeled, although these hydrogen atom contributions were not included. All other hydrogen atom contributions were calculated, but not refined. The final values of refinement parameters are given in Table 1. The locations of the largest peaks in the final difference Fourier map calculation and the magnitude of the residual electron densities in each case were of no chemical significance. Crystallographic data have been deposited as Supporting Information.

Results and Discussion

While it is generally observed that phosphazides are thermally sensitive intermediates on route to phosphinimines,^{12,13} the interceptions of phosphazides have been observed for cases in which the reagents are sterically demanding.^{14,15} Similar conclusions are illustrated by the oxidation of the phosphines R_3P , $R = i\text{-Pr}$, $t\text{-Bu}$, with the azide N_3CH_2SPh . In the case of $i\text{-Pr}_3P$, reaction with N_3CH_2SPh proceeds with the vigorous evolution of gas to afford the liquid **1** in 98% yield. This material exhibits a single ^{31}P NMR resonance at 32.8 ppm. The ^1H NMR resonances at 7.80–6.93, 5.25, 1.88, and 0.98 ppm were consistent with the presence of phenyl, methylene, methine, and methyl protons, respectively. The corresponding $^{13}\text{C}\{^1\text{H}\}$ NMR resonances were observed, consistent with the formulation of the expected product $i\text{-Pr}_3PNCH_2SPh$ **1**. In an analogous manner, the reaction of $t\text{-Bu}_3P$ under similar conditions proceeds to give a white product **2** in 73% yield (Scheme 1). This material exhibits a signal in the $^{31}\text{P}\{^1\text{H}\}$ NMR spectrum at 50.9 ppm. Similar to **1**, ^1H NMR resonances at 7.59–6.88, 5.28, and 1.17 ppm were consistent with the presence of phenyl, methylene,

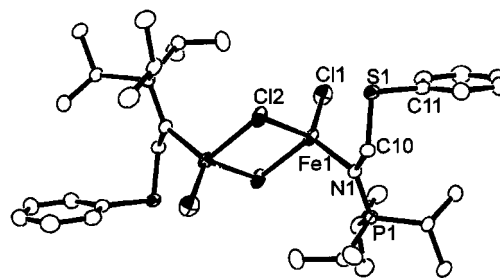


Figure 1. ORTEP drawing of **3**, 20% thermal ellipsoids are shown. Hydrogen atoms are omitted for clarity. Fe(1)–N(1) 2.033(2); Fe(1)–Cl(1) 2.2556(12), Fe(1)–Cl(2) 2.3918(10); Fe(1)–Cl(2)′ 2.4586(11); P(1)–N(1) 1.619(3); Fe(1)–S(1) 3.068(2); N(1)–Fe(1)–Cl(1) 125.74(8); N(1)–Fe(1)–Cl(2) 106.19(7); Cl(1)–Fe(1)–Cl(2) 118.25(5); N(1)–Fe(1)–Cl(2)′ 112.51(8); Cl(1)–Fe(1)–Cl(2) 99.54(5); Cl(2)′–Fe(1)–Cl(2) 87.42(3); Fe(1)–Cl(2)–Fe(1) 92.58(3); P(1)–N(1)–Fe(1) 130.36(14).

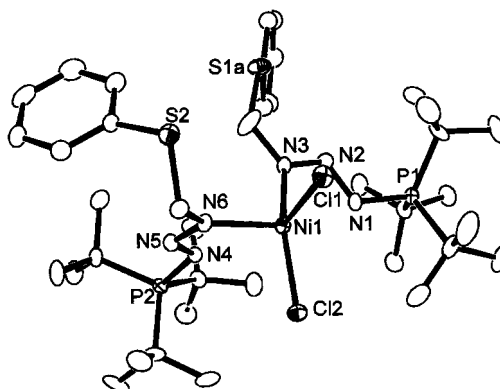


Figure 2. ORTEP drawing of **4**, 20% thermal ellipsoids are shown. Hydrogen atoms are omitted for clarity. Ni(1)–N(3) 2.017(6); Ni(1)–N(6) 2.031(6); Ni(1)–Cl(2) 2.275(2); Ni(1)–Cl(1) 2.309(2); Ni(1)–N(1) 2.635(6); Ni(1)–N(4) 2.789(6); P(1)–N(1) 1.675(6); P(2)–N(4) 1.652(6); N(1)–N(2) 1.354(8); N(2)–N(3) 1.287(8); N(4)–N(5) 1.353(8); N(5)–N(6) 1.272(7); N(3)–Ni(1)–N(6) 99.3(2); N(3)–Ni(1)–Cl(2) 152.83(18); N(6)–Ni(1)–Cl(2) 96.84(17); N(3)–Ni(1)–Cl(1) 93.22(18); N(6)–Ni(1)–Cl(1) 99.84(17); Cl(2)–Ni(1)–Cl(1) 105.40(9); N(2)–N(1)–P(1) 112.8(5); N(3)–N(2)–N(1) 109.0(5); N(2)–N(3)–Ni(1) 114.6(5); N(5)–N(4)–P(2) 115.2(5); N(6)–N(5)–N(4) 110.7(6); N(5)–N(6)–Ni(1) 118.8(4).

and *tert*-butyl groups. However, the absence of P-coupling to the methylene protons and the lack of gas evolution in this latter reaction suggest the formulation of **2** as $t\text{-Bu}_3PN_3CH_2SPh$, a view that was also supported by elemental analysis. Heating solutions of **2** to 140° results only in decomposition. Presumably, the greater steric demands of the $t\text{-Bu}_3P$ fragment precludes effective N_2 elimination and formation of the corresponding phosphinimine.

The synthesis of **1** and **2** permits a comparison of these related ligands. Reaction of compound **1** with FeCl_2 in toluene proceeds with the formation of a pale yellow precipitate, which could be extracted in dichloromethane. Upon standing, pure yellow crystalline product **3** was obtained in 21% yield. The relatively low yield was attributed to the high solubility of the complex. An X-ray structural determination confirmed the formulation of **3** as the symmetric dimeric species $[(i\text{-Pr}_3PNCH_2SPh)FeCl(\mu\text{-Cl})_2]$ **3** (Figure 1). In this species, two Fe centers are coordinated to the phosphinimine–nitrogen atom and a terminal chlorine. Two other chlorine atoms bridge the two Fe centers. The terminal and average bridging Fe–Cl distances of 2.2556(12) and 2.4252(11) Å are clearly significantly different, reflecting the different environments. The Fe–N distance of 2.033(2) Å is typical of coordinated Fe–phosphinimines.¹⁶ Comparison of the long Fe–thioether S distance of 3.068(2) Å in **3** to those in

(11) Cromer, D. T.; Mann, J. B. *Acta Crystallogr., Sect. A* **1968**, *A24*, 321–324.

(12) Staudinger, H. *Helv. Chim. Acta* **1919**, *2*, 635.

(13) Pilgram, K.; Goergen, F.; Pollard, G. *J. Heterocycl. Chem.* **1971**, *8*, 951–959.

(14) Velasco, M. D.; Molina, P.; Fresneda, P. M.; Sanz, M. A. *Tetrahedron* **2000**, *56*, 4079–4084.

(15) Kukhar, V. P.; Kasukhin, L. F.; Ponomarchuk, M. P.; Chernega, A. N.; Antipin, M. Y.; Struchkov, Y. T. *Phosphorus, Sulfur Silicon Relat. Elem.* **1989**, *44*, 149–153.

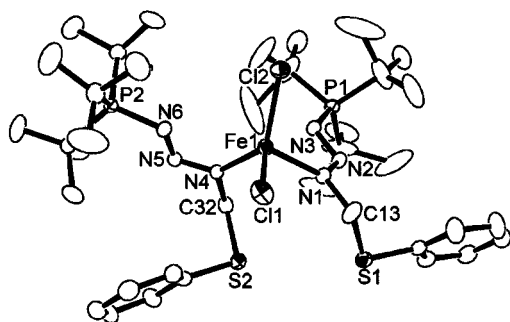


Figure 3. ORTEP drawing of **5**, 20% thermal ellipsoids are shown. Hydrogen atoms are omitted for clarity. Fe(1)–N(4) 2.076(3); Fe(1)–N(1) 2.122(3); Fe(1)–Cl(2) 2.2587(12); Fe(1)–Cl(1) 2.3093(13); P(1)–N(3) 1.650(3); P(2)–N(6) 1.660(3); N(1)–N(2) 1.273(3); N(2)–N(3) 1.330(3); N(4)–N(5) 1.288(3); N(5)–N(6) 1.309(4); N(4)–Fe(1)–N(1) 96.54(10); N(4)–Fe(1)–Cl(2) 125.80(8); N(1)–Fe(1)–Cl(2) 108.84(8); N(4)–Fe(1)–Cl(1) 108.35(8); N(1)–Fe(1)–Cl(1) 101.60(7); Cl(2)–Fe(1)–Cl(1) 111.99(5); N(2)–N(1)–Fe(1) 124.5(2); N(1)–N(2)–N(3) 112.1(2); N(2)–N(3)–P(1) 115.4(2); N(5)–N(4)–Fe(1) 123.5(2); N(4)–N(5)–N(6) 112.1(2); N(5)–N(6)–P(2) 116.6(2).

the Fe complexes $[\text{Fe}(\text{N}_2\text{H}_2\text{S}_2)]_2$ (2.572(1) Å, $\text{N}_2\text{H}_2\text{S}_2 = 2,2'$ -bis(2-mercaptophenylamino)diethyl sulfide)¹⁷ and $\text{Fe}(\text{N}_2\text{H}_2\text{S}_3)(\text{CO})$ (2.279(2) Å, $\text{N}_2\text{H}_2\text{S}_3 = 2'$ -bis(2-mercaptophenylamino)diethyl sulfide)¹⁷ suggests a very weak Fe–S interaction in **3**.

Reaction of compound **2** with either $\text{NiCl}_2(\text{DME})$ or FeCl_2 affords the paramagnetic complexes (*t*-Bu₃PN₃CH₂SPh)₂NiCl₂ **4** and (*t*-Bu₃PN₃CH₂SPh)₂FeCl₂ **5**, respectively (Scheme 1). These compounds were obtained in good yield, and each was structurally characterized by X-ray crystallography. In both complexes, the metal centers are bonded to two chlorine atoms and two nitrogen atoms of the phosphazide ligands adjacent the methylene group. The coordination of these N atoms is presumably a result of the lesser steric crowding, compared to

the P-bound N atom, and is electronically favored.^{8,18} In **4**, (Figure 2), the Ni–N and Ni–Cl distances average 2.024(6) Å and 2.292(2) Å, respectively. The two phosphorus-bound nitrogen atoms also approach the Ni center at distances of 2.635(6) and 2.789(6) Å, presumably as a result of a weak chelate effect. In a similar manner, the two Fe–N and Fe–Cl distances of complex **5**, (Figure 3), average 2.101(4) and 2.2840(14) Å, respectively. The closest approaches of the P-bound N atoms to Fe are 3.024(6) and 2.971(6) Å. The longer range metal–nitrogen in **4** and **5** may reflect weak interactions that contribute to distortions about the metal coordination spheres. For example, the angles about Fe in **5** range from 96.54(10)° to 125.80(8)°. The nature of binding of the phosphazide ligands in **4** and **5** stands in contrast to that seen in $\text{WBr}_2(\text{CO})_3(\text{ArN}_3\text{PPh}_3)$, in which the phosphazide acts as a bidentate ligand with similar W–N bond lengths (2.163(4), 2.220(5) Å).⁷

The synthesis of the phosphinimine **1** and phosphazide **2** confirms that steric issues must be considered in developing a synthetic strategy to bidentate phosphinimine ligands. Moreover, the crystallographic data for the Fe and Ni complexes **3**–**5** suggest that chelation via the thioether S or a phosphazide N atom exhibits only a weak stereochemical effect on a metal center. These data suggest that synthetic routes to bidentate ligands derived from phosphinimines may require the incorporation of both stronger secondary donors and longer donor atom separations to permit effective chelation. Strategies to such ligands are under development.

Acknowledgment. Financial support from the NOVA Chemicals Corporation and NSERC of Canada is gratefully acknowledged.

Supporting Information Available: Crystallographic X-ray crystallographic files in CIF format for the structure determinations of compounds **3**–**5**. This material is available free of charge via the Internet at <http://pubs.acs.org>.

IC001303X

(16) Mai, H. J.; Wocadlo, S.; Kang, H. C.; Massa, W.; Dehnicke, K.; Maichle-Moessner, C.; Straehle, J.; Fenske, D. *Z. Anorg. Allg. Chem.* **1995**, 621, 705–712.

(17) Sellmann, D.; Utz, J.; Heinemann, F. W. *Inorg. Chem.* **1999**, 38, 459–466.

(18) Widauer, C.; Grutzmacher, H.; Shevchenko, I.; Gramlich, V. *Eur. J. Inorg. Chem.* **1999**, 1659–1664.